Catal Lett (2009) 128:9–17
DOI 10.1007/s10562-008-9802-0

Investigation of Ethylene Oxide on Clean and Oxygen-Covered Ag(110) Surfaces

A. C. Lukaski · Mark A. Barteau

Received: 22 August 2008 / Accepted: 30 November 2008 / Published online: 13 December 2008

Abstract Temperature-programmed desorption (TPD) and Density Functional Theory (DFT) were used to investigate the reactions of oxametallacycles derived from ethylene oxide on clean and oxygen-covered Ag(110) surfaces. Ethylene oxide ring-opens following adsorption at 250 K on both clean and O-covered Ag(110) to form a stable oxametallacycle. On the clean Ag(110) surface, the oxametallacycle reacts to reform the parent epoxide at 280 K during TPD, while the aldehyde isomer, acetaldehyde, is observed at higher oxametallacycle coverages. In the presence of coadsorbed oxygen atoms, a portion of the oxametallacycles dissociate to release ethylene. However, of those that react to form oxygen-containing products, the fraction forming ethylene oxide is similar to that on the clean surface. The acetaldehyde product of oxametallacycle reactions combusts via formation of acetate species; the acetates react to form CO_2 at temperatures as low as 360 K on the O-covered surface. No evidence was observed for other combustion channels. This work provides experimental evidence for the connection of oxametallacycles to combustion via acetaldehyde formation as well as to ring-closure to form ethylene oxide.

Keywords Ethylene oxide · Oxametallacycle · Silver · Temperature-programmed reaction · Density Functional Theory · Olefin epoxidation catalysis

1 Introduction

The direct, silver-catalyzed epoxidation of ethylene to ethylene oxide has been the focus of considerable study [1]. Ethylene oxide is the largest volume compound produced by the chemical process industry via selective oxidation, with annual production valued at close to $9 billion USD (>$1.4 \times 10^{10}$ kg) [2]. Despite over 70 years of industrial practice, the mechanism of the reaction remained obscure until recently [3–9], and the majority of significant advances in Ag-catalyst development occurred primarily through empirical approaches [10]. Silver, however, remains the cornerstone of commercial catalysts for ethylene oxide production due to its unique ability to selectively epoxidize ethylene with high selectivity. With the exception of the small-scale commercial production (now discontinued) of epoxybutene via Ag-catalyzed epoxidation of 1,3-butadiene by Eastman Chemical, ethylene oxide is the only epoxide generated by direct, heterogeneous oxidation on an industrial scale [11].

Earlier surface science studies [12–20] of Ag-catalyzed ethylene epoxidation primarily addressed the roles of oxygen and promoters. By the late 1980s, a reasonable consensus emerged that addition of atomic, rather than molecular, oxygen to the double bond of ethylene led to epoxide formation. If molecular oxygen were the active species for epoxidation, a maximum selectivity to ethylene oxide of 6/7 would be expected because six molecules of O_2 would yield six molecules of ethylene oxide and six oxygen atoms; a seventh ethylene molecule would be required to consume the remaining six oxygen atoms by reaction to CO_2 and water. Molecular oxygen cannot be the active species for epoxidation, however, as selectivities over 90% to ethylene oxide have been reported [12].

A. C. Lukaski · M. A. Barteau (✉)
Department of Chemical Engineering, Center for Catalytic Science and Technology, University of Delaware, Newark, DE 19716, USA
e-mail: barteau@udel.edu; barteau@che.udel.edu

Molecular-level understanding of epoxidation has been limited by difficulty in probing reacting species on the catalyst surface. Because the kinetically significant steps occur early in the reaction sequence, surface intermediates that form epoxide products directly are not easily identified on working catalysts [4]. In surface science studies under ultra-high vacuum (UHV) conditions, ethylene desorbs from silver at temperatures below those required for reaction with adsorbed oxygen. Linic and Barteau [4] concluded that *both* dissociative adsorption of oxygen and addition of oxygen atoms to weakly adsorbed ethylene were kinetically relevant steps in the steady-state catalytic mechanism; either of these steps could be rate-determining depending on reaction conditions. Subsequent steps, however, did not affect the overall rate of reaction.

Surface science and computational studies [3–9] have circumvented these limitations and have identified the central intermediate in epoxidations of both ethylene and butadiene by examination of the reverse reactions. This intermediate is a surface oxametallacycle that can be formed in UHV experiments by opening the epoxide ring. The oxametallacycle controls the selectivity of epoxidation through competing steps: ring-closure to form the epoxide and isomerization to aldehyde species. The aldehyde has been proposed as the gateway species to combustion products [21]. Stable, spectroscopically verified oxametallacycles have been synthesized from 2-iodo-ethanol on Ag(110) [22] and Ag(111) [6, 23], ethylene oxide on Ag(111) [3], epoxybutene on Ag(110) [5] and Ag(111) [8], and styrene oxide on Ag(110) [24] and Ag(111) [9].

Ring opening of epoxides to form oxametallacycles on silver is an activated process. On Ag(111), surface temperatures of ca. 250 K were shown to be necessary to ring-open ethylene oxide and form a stable oxametallacycle without subsequent rapid reaction of this species [3]. The oxametallacycle reacted during temperature-programmed experiments to reform the parent epoxide near 300 K, in addition to forming small amounts of products including ethanol and ethylene. The vibrational spectrum of the stable oxametallacycle was in good agreement with that calculated using Density Functional Theory (DFT) and, moreover, was remarkably similar to that of an unidentified species observed by Force and Bell [25] in steady-state reactions over supported silver. The identification of the ethylene oxide-derived oxametallacycle species [3] represents the first time that an organic intermediate in ethylene epoxidation was isolated and characterized experimentally.

The present study investigates the interaction of ethylene oxide with the Ag(110) surface and demonstrates the formation of an oxametallacycle intermediate by activated ring-opening of the epoxide on both clean and O-covered Ag(110) surfaces. Unlike our previous studies of oxametallacycle chemistry on oxygen-free surfaces, the results of this work provide insights into the influence of oxygen, which is present on working catalysts, on various steps in the reaction network.

Several previous studies have examined epoxide reactions in the presence of co-adsorbed oxygen. Bare [26] investigated the adsorption of ethylene oxide on the clean and O-covered Ag(110) surfaces and found that ethylene oxide adsorbed weakly on the clean surface. Adsorption of ethylene oxide at 90 K led to molecular desorption at 120 and 160 K during subsequent TPD. In the presence of co-adsorbed oxygen, the ethylene oxide heat of adsorption increased by 30% and the epoxide desorbed from the Ag(110) surface near 200 K. The low temperatures required to prevent molecular ethylene oxide desorption, however, were insufficient to cause ring opening of the epoxide on either clean or oxygen-containing surfaces. Liu et al. [27] investigated the reactions of styrene, styrene oxide, and phenylacetaldehyde on clean and O-covered Ag(110) surfaces. These authors found that reactions of styrene oxide and phenylacetaldehyde on the O-covered Ag(110) surface led to similar products to those from styrene reaction with adsorbed oxygen. They concluded that styrene undergoes epoxidation through an oxametallacycle intermediate.

Based on DFT calculations, Kokalj et al. [28] also concluded that the adsorption of ethylene on an atomic oxygen-covered Ag(100) surface led to the formation of an oxametallacycle. At low oxygen coverages ($\theta_O \leq 0.5$ ML), the authors found a weak dependence of the ring-closure activation barrier on oxygen coverage. At high oxygen coverages on Ag(100), oxygen atoms bind less strongly to the surface and, hence, are more easily incorporated into the oxametallacycle. However, high oxygen coverages also reduce the carbon-metal bond strength of the oxametallacycle due to competition for surface sites between the oxametallacycle and oxygen. These two interactions effectively cancel each other and, therefore, the activation barrier calculated for oxametallacycle formation is only weakly dependent on the oxygen coverage [28]. Bocquet and Loffreda [29] studied the reactions of ethylene oxide oxametallacycles on the Ag(111) surface using DFT and found two types of oxygen species on the surface: a low coverage atomic phase and an oxide overlayer. In agreement with Kokalj et al. [28], the authors found that the computed reaction pathways and activation barriers were similar at all oxygen coverages.

The combination of temperature-programmed reaction techniques with DFT was used in the present work to identify the oxametallacycle species derived from ethylene oxide on Ag(110). On the clean Ag(110) surface, the oxametallacycle reacts to reform the parent epoxide at 280 K; the aldehyde isomer, acetaldehyde, is formed at higher oxametallacycle coverages. On the O-covered Ag(110) surface, the oxametallacycle exhibits moderately lower selectivity to the epoxide than on the clean surface and undergoes combustion through formation of acetaldehyde and acetate species. While the structure of the reaction network is not surprising, the connection of oxametallacycles to combustion has not previously been established in surface science studies.

2 Experimental and Theoretical Methods

2.1 Surface Science Experiments

Temperature-programmed desorption (TPD) experiments were conducted in a VG Mark II ESCALAB chamber that was equipped with diffusion and ion pumps. After heating or cooling to the desired temperature, the adsorbate was dosed onto the crystal surface via a 1/16″ diameter stainless steel line placed ~1 cm from the crystal face; note that the reported exposures are based on the background pressure and do not account for the enhancement effect of the direct doser. The crystal was then positioned under the aperture in the mass spectrometer shroud and heated linearly at 3 K/s in all experiments using a high stability temperature controller (Eurotherm 2404f). Mass fragmentation patterns were obtained experimentally by backfilling the chamber with the pure component and collecting mass spectral scans up to m/q = 200. The quantitative product distribution was determined using the method of Ko et al. [30] and was based on the cracking pattern measurements with the same instrument used to record TPD spectra. Cracking patterns were measured for ethylene oxide (Aldrich, 99.5+%), ethanol (Sigma Aldrich, 99.5+%), ethylene (Keen, 99.5+%), and acetaldehyde (Sigma Aldrich, 99.5+%) after successive freeze-pump-thaw cycles removed any residual contaminants from those reagents that were stored as liquids under ambient conditions.

Alternating argon-ion bombardment and annealing cycles to 750 K removed impurities from the sample surface, and oxygen TPD established surface cleanliness prior to ethylene oxide TPD experiments.

2.2 Computational Methods

The Amsterdam Density Functional (ADF) [31–33] program was used to determine the total energies and fully optimized geometric structures of oxametallacycle intermediates on isolated Ag clusters. Heats of reaction for oxametallacycle formation were calculated using Eq. 1 from the energies of the oxametallacycle bound to a silver cluster and the energies of the bare cluster and the free ethylene oxide molecule.

$$\Delta H_{Rxn} \approx \Delta E_{Rxn} = E(\text{oxametallacycle}) - \{E(\text{EO}) + E(\text{M}_\text{n})\} \quad (1)$$

The terms $E(\text{EO})$ and $E(\text{M}_\text{n})$ represent the respective total energies of the optimized free epoxide and the bare metal cluster composed of n silver atoms. For the calculations reported in this work, a seven-atom silver cluster was used, and thus n = 7. Subsequent optimization of geometries on periodic slabs (DACAPO source code) verified the absence of artifacts arising from the use of a terminated cluster model of the Ag surface.

3 Results

3.1 Temperature-Programmed Desorption

3.1.1 Ethylene Oxide Adsorption on Clean Ag(110)

Following adsorption at 120 K on Ag(110), ethylene oxide desorbed near 140 and 160 K. Figure 1 shows the m/q = 29 TPD signal used to monitor ethylene oxide desorption following adsorption of 0.005L of ethylene oxide at 120 K. The higher temperature feature at 160 K saturated with larger ethylene oxide doses and is attributed to desorption from the monolayer state, while the lower temperature state at 140 K continued to increase with exposure and is attributed to the multilayer state. Bare [26] also identified a peak at 160 K as molecular ethylene oxide desorption from the monolayer state following adsorption of the epoxide at 90 K on the clean Ag(110) surface. Similarly, adsorption of ethylene oxide at 90 K on the Ag(111) surface led to desorption at 130 and 200 K with a small feature near 300 K during subsequent TPD [3].

Following adsorption of ethylene oxide at 250 K, a feature at ~280 K was observed during TPD. Figure 2 shows the TPD spectra of ethylene oxide adsorbed at 250 K on the Ag(110) surface. Ethylene oxide exposure

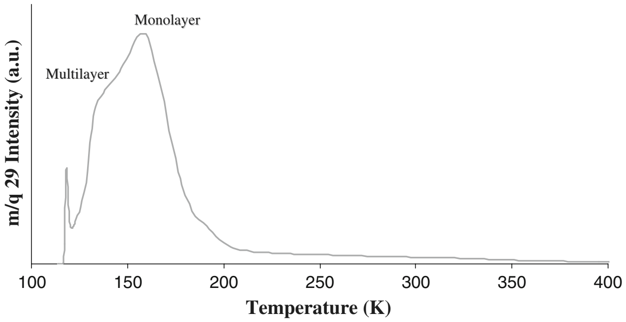

Fig. 1 TPD spectrum of ethylene oxide (monitored through m/q 29) following adsorption of ethylene oxide at 120 K on Ag(110): ethylene oxide exposure = 0.005L

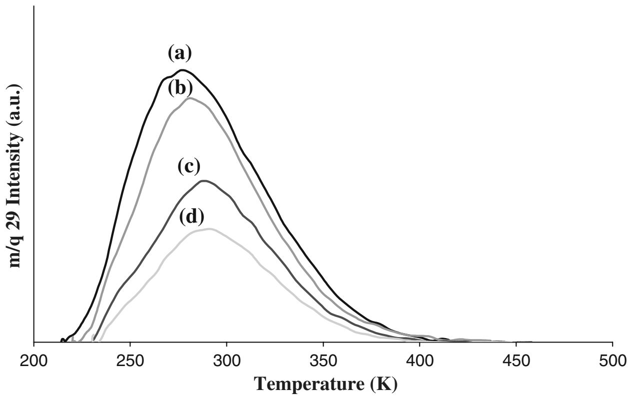

Fig. 2 m/q 29 TPD spectra following ethylene oxide adsorption at 250 K on Ag(110): ethylene oxide exposure—(a) 10L, (b) 5L, (c), 0.5L, and (d) 0.1L

was begun at 260 K and the crystal surface cooled to 240 K at the termination of the dose. During the subsequent evacuation of the chamber, the crystal temperature decreased to ~200 K. To remove the molecular ethylene oxide species that adsorbed during this time, the crystal was then flashed to 230 K and allowed to cool briefly again before initiation of the TPD ramp, The aim of this procedure was to isolate the peak at ~280 K as much as possible for coverage and composition analysis, rather than quantitative determination of the kinetics. In particular, the partial flash step may influence both the leading edge of the peak and the resultant peak position, and makes inferences about peak shape or peak shifts dubious. However, without this step, it was difficult to achieve the desired separation of the 280 K peak from the molecular states in the vacuum system used for these experiments. Wu et al. [34] previously reported that molecularly adsorbed ethylene oxide on the Ag(111) surface desorbed below 230 K. The population of the 280 K state by adsorption at higher temperatures suggests that there is an activation barrier associated with the formation of the intermediate that reforms ethylene oxide at this temperature in Fig. 2. Linic and Barteau [3] observed similar behavior following adsorption of ethylene oxide on the Ag(111) surface at 250 K and attributed the subsequent evolution of ethylene oxide at 300 K during TPD to reaction of an oxametallacycle intermediate.

Previous surface science studies [3, 5, 9, 24] generated strongly-bound oxametallacycle intermediates by ring-opening epoxides on Ag surfaces and reported that activation of this process required adsorption at surface temperatures above 200 K; the oxametallacycles underwent ring-closure during TPD to reform the parent epoxides at temperatures well above those reported for desorption of the molecular epoxide states. The similar surface chemistry of the intermediate derived from ethylene oxide on Ag(110) to that of the oxametallacycle formed from ethylene oxide on Ag(111) suggests that the species formed on the Ag(110) surface is also an oxametallacycle.

In keeping with the previous determinations of activation energies for oxametallacycle reactions and the comparisons of these to DFT calculations [24] a Redhead analysis based on the peak temperature was used to determine an activation barrier of 18 kcal/mol for formation of ethylene oxide from the oxametallacycle intermediate species on Ag(110). The analysis used a pre-exponential factor of 10^{13} s^{-1} for a first-order process. This approach permits consistent comparison of the barriers for reactions of different oxametallacycle species on different surfaces. The peak shapes for reaction of epoxybutene-derived and styrene oxide-derived oxametallacycles at higher temperatures on Ag(111) and (110) surfaces are consistent with first order processes [5, 8, 9, 24], but those for EO-derived oxametallacycles are less consistent owing to the procedures for isolating these peaks from the molecular state, as noted above. Nevertheless, the barriers determined are consistent with DFT calculations and previous results on the (111) surface. The DFT-calculated heat of reaction for forming the oxametallacycle from the free ethylene oxide molecule on the bare Ag(110) surface is 7 kcal/mol. Figure 3 shows the DFT-predicted oxametallacycle structure derived from ethylene oxide on a seven-atom truncation of the Ag(110) surface; note that the ethylene oxide-derived oxametallacycle adopts a similar geometry when the oxygen atom is bound to the terminal Ag atom or the seven-atom representation of the Ag(110) surface. Combining the experimental activation barrier for oxametallacycle ring-closure and epoxide formation with the DFT-predicted heat of reaction leads to a ring-opening activation barrier of 11 kcal/mol. This value is in excellent agreement with that reported for ring-opening the epoxide on the Ag(111) surface. Linic and Barteau [3] reported activation barriers of 17 and 11 kcal/mol for the respective ring-closure and ring-opening reactions of the oxametallacycle intermediate on the Ag(111) surface. Previous studies of epoxybutene reported similar activation barriers for ring-opening that epoxide on the Ag(111) [9] and Ag(110) [5] surfaces as well.

The product distributions in the ethylene oxide TPD spectra were determined by comparing the mass fragmentation pattern from eight principal masses with the cracking patterns of ethylene oxide (EO), acetaldehyde (AcA), ethylene (Et), and ethanol (EtOH). Little variation of the peak shapes was observed for these masses, indicative of nearly coincident evolution of the products that give rise to them. Table 1 shows the gas-phase cracking patterns of these species relative to the m/q 28 signal for each. In addition to ethylene oxide, acetaldehyde was also formed during TPD following adsorption of larger amounts of ethylene oxide at 250 K on the clean surface. The relative product

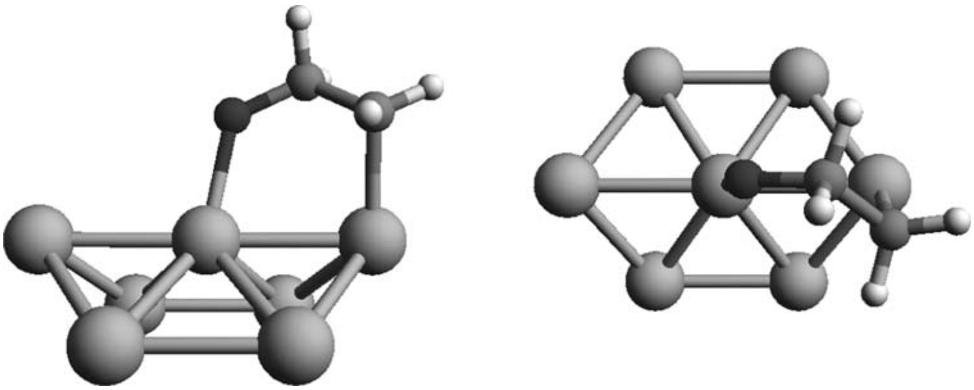

Fig. 3 Optimized ethylene oxide-derived oxametallacycle structure on 7-atom truncation of the Ag(110) surface

Table 1 Gas-phase cracking patterns of ethylene oxide, acetaldehyde, ethylene, and ethanol expressed relative to m/q 28

Species	Mass-to-charge (m/q)							
	14	15	27	28	29	42	43	44
Ethylene oxide	0.64	1.41	0.26	1.00	1.64	0.52	0.75	1.58
Acetaldehyde	0.86	1.86	0.18	1.00	2.79	0.73	1.81	2.54
Ethylene	0.07	0.01	0.84	1.00	0.00	0.00	0.00	0.00
Ethanol	0.17	0.33	0.67	1.00	0.79	0.14	0.30	0.32

Table 2 Product distribution (monolayers, ML) from TPD of ethylene oxide adsorbed at 250 K on clean Ag(110)

EO dose (L)	Coverage (ML) θ_{OME}	Yields				EO selectivity S (%)
		Y_{EO}	Y_{AcA}	Y_{Et}	Y_{EtOH}	
0.5	0.26	0.18	0.08	0.00	0.00	69
1	0.37	0.25	0.12	0.00	0.00	68
5	0.39	0.26	0.13	0.00	0.00	67
10	0.45	0.29	0.16	0.00	0.00	64

contributions to the peak areas for the eight masses sampled were determined via least squares error minimization of a series of linear equations incorporating product cracking patterns. Table 2 summarizes the product distributions from the TPD spectra obtained following adsorption of different exposures of ethylene oxide at 250 K on the clean Ag(110) surface. Oxametallacycle surface coverages (θ_{OME}), reported in monolayers (ML), were calibrated against the saturated TPD trace for desorption of oxygen from Ag(110) at 570 K (not shown). The oxygen TPD peak saturates at a coverage of 0.5 ML. Yields were determined using the method of Ko et al. [30] from the total product distribution by calculating mass spectrometer sensitivity factors from the cracking pattern of each product. The total coverage of oxametallacycles on the surface was equated with the sum of yields of C_2-containing products.

Increasing the oxametallacycle coverage on the Ag(110) surface decreased the selectivity to ethylene oxide only slightly (Table 2). The selectivity to ethylene oxide decreased from 69% to 64% as the oxametallacycle coverage increased from 0.26 to 0.45 ML; the oxametallacycle coverage saturated at ca. 0.5 ML on the clean Ag(110) surface. Oxametallacycles formed from ring-opening of styrene oxide on Ag(110) exhibited a similar trend, with decreasing selectivity to the epoxide as the oxametallacycle coverage increased [24]. The ethylene oxide yield (Y_{EO}) increased with coverage, as the increasing oxametallacycle coverage (θ_{OME}) more than compensated for the apparent selectivity decrease (Table 2).

3.1.1.1 Ethylene Oxide Adsorption on O-Covered Ag(110) Figure 4 shows the m/q 29 TPD spectra of ethylene oxide adsorbed on the O-covered Ag(110) surface. Prior to ethylene oxide adsorption, the Ag(110) surface was exposed to a saturation dose of oxygen above 300 K to produce a 0.5 ML coverage of oxygen atoms. As for the previous experiments on oxygen-free surfaces, ethylene oxide was dosed onto the crystal surface as the surface cooled down and the surface was then flashed to remove molecularly adsorbed species. Similar to adsorption on the clean Ag(110) surface, the oxametallacycle reacted to reform the parent epoxide at 280 K. In addition, carbon dioxide desorption was observed near 350 and 450 K (Fig. 5). Table 3 summarizes the product distribution following ethylene oxide adsorption on the O-covered Ag(110) surface, as well as the amount of unreacted oxygen that desorbed during TPD. The selectivities to ethylene oxide were ca. 10–20% lower on the O-covered surface than on the clean Ag(110) surface throughout the range of coverages explored.

At the highest oxametallacycle coverages, the yield of ethylene oxide was approximately 20% lower on the oxygen-covered surface than on the clean surface, although the oxametallacycle coverage was approximately 40% higher on this surface. The higher coverage suggests that the presence of oxygen decreases the activation barrier for oxametallacycle formation on the Ag(110) surface or

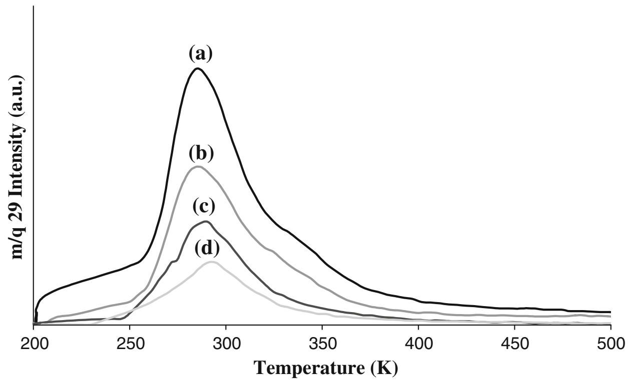

Fig. 4 m/q 29 TPD spectra following adsorption of ethylene oxide at 250 K on oxygen-covered Ag(110): ethylene oxide exposure—(a) 10L, (b) 5L, (c), 0.5L, and (d) 0.1L

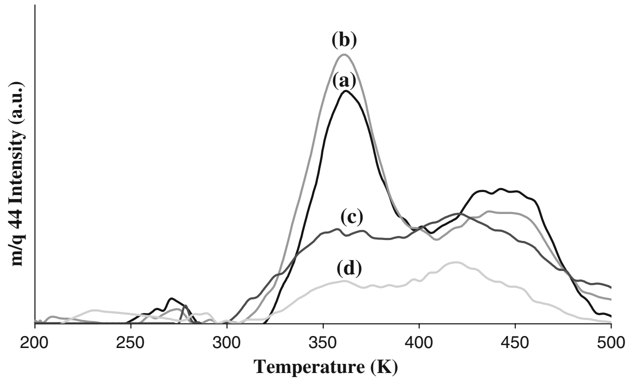

Fig. 5 m/q 44 TPD spectra following adsorption of ethylene oxide at 250 K on oxygen-covered Ag(110): ethylene oxide exposure—(a) 10L, (b) 5L, (c) 0.5L, and (d) 0.1L

increases the capacity of the surface. Guo and Madix [35] reported that the Ag(110) surface undergoes a 1 × 2 reconstruction when exposed to high doses of oxygen. This suggests that saturation of the Ag(110) surface with oxygen may also increase the capacity of the surface. No acetaldehyde desorption was observed from the O-covered surface. Instead, the principal side products were ethylene and CO_2. The appearance of ethylene suggests that the presence of coadsorbed oxygen may increase the reverse of the epoxidation reaction from the oxametallacycle to ethylene and oxygen.

In order to determine whether CO_2 formation occurs via acetaldehyde combustion in the reaction of ethylene oxide-derived oxametallacycles on the O-covered Ag(110) surface, the reaction of small amounts of acetaldehyde on the surface was also examined. Figure 6 shows the m/q 44 trace used to monitor carbon dioxide desorption during acetaldehyde TPD on the O-covered Ag(110) surface. At higher acetaldehyde coverages, CO_2 evolution occurred only from a high-temperature state near 630 K; this temperature is characteristic of decomposition of an acetate species on an oxygen-free surface [36]. At lower acetaldehyde coverages, however, CO_2 is produced primarily from lower-temperature channels near 350 and 400 K. Sault and Madix [37] found that acetate reacts with adsorbed oxygen atoms on Ag(110) at low coverages to make formate. Adsorbed formate then decomposes and CO_2 desorbs at 375 K during TPD. As the acetate coverage increases, a new CO_2 peak forms at 400 K and, when surface oxygen is depleted, CO_2 is released primarily from the high temperature acetate decomposition channel above 600 K.

Figure 7 compares CO_2 production from acetaldehyde and ethylene oxide TPD following adsorption at 250 K on O-covered surfaces. Similar CO_2 desorption traces were observed during reactions of both acetaldehyde and ethylene oxide with the O-covered surface. These observations clearly illustrate a common signature characteristic of the reaction between acetate and surface oxygen. Further, they demonstrate that acetate formation from either oxametallacycles or acetaldehyde species must be complete by ~320 K, the onset temperature for CO_2 production. Since the peak temperature for oxametallacycle reaction to ethylene oxide and acetaldehyde is 280 K, the formation of acetate from oxametallacycles via oxidation of acetaldehyde species is quite feasible. Linic and Barteau [4] mapped out the reaction coordinate for ethylene epoxidation on Ag(111) and concluded that the selectivity of the reaction is controlled by competing reactions of the oxametallacycle: ring-closure yields ethylene oxide and isomerization to acetaldehyde leads to combustion. However, direct experimental evidence connecting the oxametallacycle to combustion via acetaldehyde was previously lacking.

Table 3 Product distribution (monolayers, ML) from TPD of ethylene oxide adsorbed at 250 K on oxygen-covered Ag(110)

EO dose (L)	Coverage (ML)		Yields					EO selectivity
	θ_O, unreacted	θ_{OME}	Y_{CO_2}	Y_{EO}	Y_{AcA}	Y_{Et}	Y_{EtOH}	S (%)
0.1	0.50	0.14	0.02	0.08	0.00	0.03	0.01	62
0.5	0.40	0.23	0.07	0.10	0.00	0.03	0.03	53
5	0.16	0.40	0.04	0.20	0.00	0.11	0.05	53
10	0.17	0.70	0.11	0.24	0.00	0.17	0.18	38

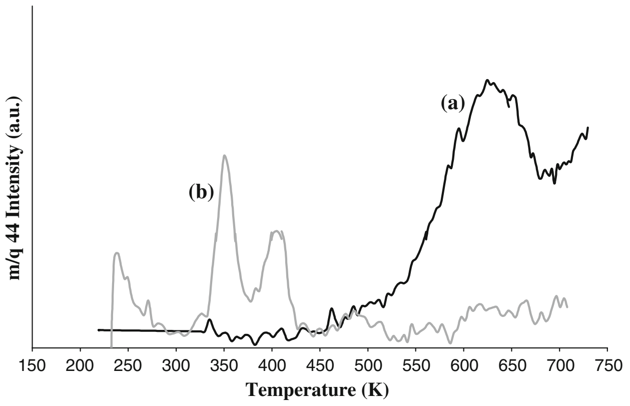

Fig. 6 m/q 44 TPD spectra following adsorption of acetaldehyde at 250 K on oxygen-covered Ag(110): acetaldehyde exposure—(a) 0.2L and (b) 0.005L

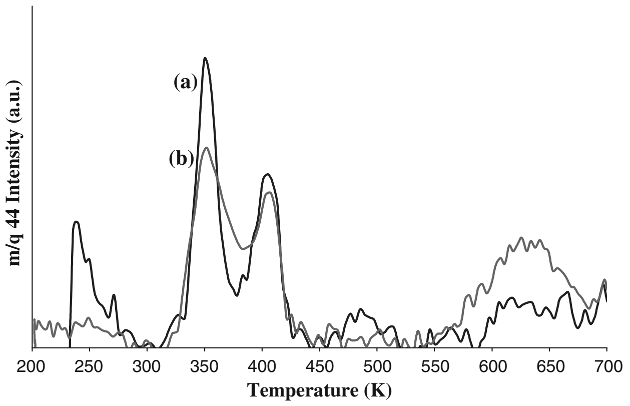

Fig. 7 m/q 44 TPD spectra following adsorption of (a) acetaldehyde (0.005L) and (b) ethylene oxide (1L) at 250 K on oxygen-covered Ag(110)

4 Discussion

The ethylene oxide-derived oxametallacycle formed on Ag(110) is consistent with the family of previously identified oxametallacycles on Ag surfaces. The formation of oxametallacycles from epoxides is an activated process that requires adsorption at surface temperatures above 200 K. Isomerization of the oxametallacycle via intra-molecular hydrogen transfer leads to the formation of aldehyde species and competes with ring-closure and reformation of the parent epoxide. Ethylene oxide-derived oxametallacycles undergo ring-closure near room temperature on both Ag(111) and Ag(110) surfaces with activation barriers for ring-closure of 17–18 kcal/mol.

The presence of coadsorbed oxygen on Ag(110) may increase the capacity of the surface through formation of metal oxide layer, as high oxygen coverages lead to a 1 × 2 reconstruction [35]. This may help to explain the higher oxametallacycle coverage on this surface; the oxametallacycle coverage was approximately 40% higher on the O-covered surface compared to that on the clean Ag(110) surface. Bare [26] reported a 30% increase in the ethylene oxide heat of adsorption in the presence of oxygen on Ag(110), while Stacchiola et al. [38] found that the heats of ethylene and ethylene oxide adsorption on Ag(111) also increased in the presence of pre-adsorbed oxygen. Backx et al. [39] reported that the ethylene oxide saturation coverage was enhanced by the presence of coadsorbed oxygen on the Ag(110) surface. The activation barrier for oxametallacycle ring-closure, however, was not affected by the presence of oxygen, as ethylene oxide was produced at the same temperatures on both the O-covered and clean Ag(110) surface. The DFT calculations of Bocquet et al. [40] also showed that the activation barrier for oxametallacycle ring-closure on Ag(111) was not significantly changed by the presence of co-adsorbed oxygen.

The principal impact of coadsorbed oxygen on the selectivity of oxametallacycle conversion to ethylene oxide appears to be the promotion of the reverse reaction from the oxametallacycle to ethylene and oxygen, rather than perturbation of the ring-closure/isomerization reaction rates, as the activation barriers for ring-closure were the same on both surfaces. Stacchiola et al. [38] reported that the presence of coadsorbed oxygen ($\theta \sim 0.1$ ML) increased the binding of ethylene on the Ag(111) surface. Backx et al. [41] reported that the activation barrier for ethylene desorption from the clean Ag(110) surface increased from 9 to 12.5 kcal/mol on the O-covered Ag(110) surface. The observation of ethylene production from ethylene oxide on the O-covered surface, but not on the clean surface, suggests that the presence of oxygen must also reduce the barrier to ethylene release from the oxametallacycle. Wu et al. [34] found that ethylene oxide underwent decomposition to ethylene and oxidation products on the O-covered Ag(111) surface. As noted above, while oxygen also increases the heat of adsorption of ethylene oxide and acetaldehyde on Ag(110) and Ag(111) surfaces [26, 38], there is little evidence for alteration of the activation barriers for the formation of these products from oxametallacycles, either from our TPD results, or from previous DFT calculations [40]. Indeed, if one omits ethylene from the determination of oxametallacycle reaction selectivities, the fraction of oxametallacycles reacted to ethylene oxide relative to the total reacting to oxygen-containing products is essentially the same on both the clean and O-covered surfaces. This is consistent with the conclusion that ethylene oxide selectivity is controlled by competing reactions of the oxametallacycle, and that CO_2 is formed by combustion of acetaldehyde produced from the oxametallacycle. The results of the present study provide no evidence for oxygen attack on ethylene oxide or on the oxametallacycle. The kinetics and selectivity of CO_2 formation can be accounted for entirely by the secondary reactions of the acetaldehyde product.

Figure 8 illustrates the effect of oxygen on the reaction coordinate in schematic form. As noted above, the comparable peak temperatures for oxametallacycle reaction on Ag(111), Ag(110), and O-Ag(110) surfaces, along with DFT calculations, suggest that the heat of reaction to form this species from gas phase ethylene oxide is insensitive to surface structure and oxygen content. Therefore, one can assess shifts in barrier heights and adsorbed states relative to the oxametallacycle. Activation energy values for both Ag(111) and Ag(110) surfaces are included in Fig. 8 since a complete set is not available for either surface in the literature. However, the observed insensitivity to surface structure in both single crystal and DFT results suggests that equating the two surfaces is a reasonable approximation in trying to understand the effects of coadsorbed oxygen on reactions on either surface.

The key point illustrated in Fig. 8 is that, while the “forward” reactions of the oxametallacycle are not affected significantly by the presence of oxygen, the “reverse” reaction to ethylene plus oxygen is affected. In order for the barriers for ethylene, ethylene oxide, and acetaldehyde reactions to become comparable, the barrier for the “reverse” reaction would need to be decreased by ca. 6 kcal/mol on the oxygen covered surface. This value compares to that for the increased heat of adsorption on O-covered surfaces reported by Stacchiola et al. [38] (2 kcal/mol). Backx et al. [39, 41] reported similarly that the presence of coadsorbed oxygen on Ag(110) promoted ethylene adsorption significantly; the activation barrier for ethylene desorption increased from 9 kcal/mol on clean Ag(110) to 12.5 kcal/mol on the O-covered surface. Based on electron energy loss spectra, the authors suggested that the amount of ethylene adsorbed on the O-covered surface increased on the order of 13 times. In summary, the effect of surface oxygen on the kinetics of the interconversion of ethylene and oxametallacycles appears to be greater than on the reactions of oxametallacycles to oxygen-containing products, including ethylene oxide.

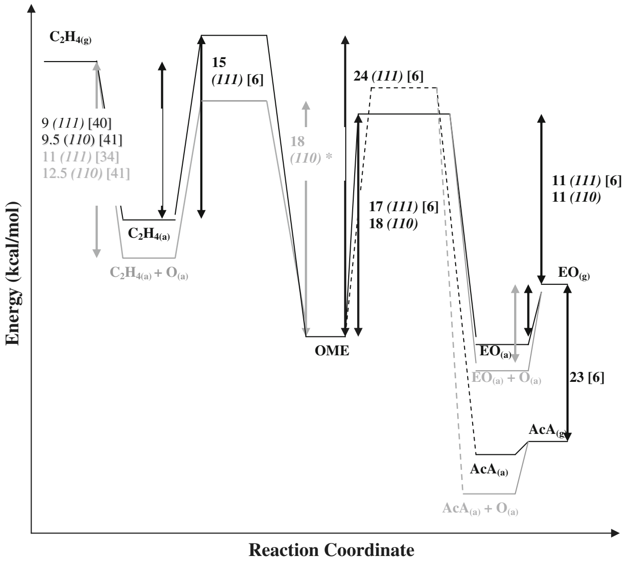

Fig. 8 Reaction coordinate of ethylene oxide-derived oxametallacycles on the clean (*black lines*) and oxygen-covered (*gray lines*) Ag surfaces

5 Conclusions

Adsorption of ethylene oxide at 250 K on both the clean and O-covered Ag(110) surfaces leads to the formation of stable oxametallacycles. The selectivity to ethylene oxide decreases with increasing oxametallacycle coverage on the clean Ag(110) surface. The presence of coadsorbed oxygen on Ag(110) decreases the selectivity to ethylene oxide and also opens combustion pathways. Combustion occurs through oxidation of the acetaldehyde product to form acetate species. These acetate species then react with oxygen to release CO_2 at temperatures as low as 350 K on the O-covered Ag(110) surface. No evidence for alternative combustion pathways was observed.

Acknowledgement We gratefully acknowledge the support of the US Department of Energy, Chemical Sciences Program, Grant FG02-84ER13290 for this research.

References

1. Van Santen RA, Kuipers HPCE (1987) Adv Catal 35:265
2. Dever JP, George KH, Hoffman WC, Soo H (2004) Kirk-Othmer encyclopedia of chemical technology, vol 10. Wiley, New York, p 632
3. Linic S, Barteau MA (2002) J Am Chem Soc 124:310
4. Linic S, Barteau MA (2003) J Catal 214:200
5. Medlin JW, Barteau MA, Vohs JM (2000) J Mol Catal A Chem 163:129
6. Linic S, Medlin JW, Barteau MA (2002) Langmuir 18:5197
7. Medlin JW, Barteau MA (2001) J Phys Chem B 105:10054
8. Enever MCN (2006) PhD Dissertation, University of Delaware
9. Enever M, Linic S, Uffalussy K, Vohs JM, Barteau MA (2005) J Phys Chem B 109:2227
10. Serafin JG, Liu AC, Seyedmonir SR (1998) J Mol Catal A Chem 131:157
11. Denton DF, Falling S, Monnier JR, Stavinoha J, Watkins W (1997) Chim Oggi-Chem Today 14:17
12. Campbell CT, Koel BE (1985) J Catal 92:272
13. Campbell CT (1985) J Catal 94:436
14. Campbell CT (1985) J Phys Chem 89:5789
15. Campbell CT (1986) J Catal 99:28
16. Campbell CT, Daube KA (1987) J Catal 106:301
17. Grant RB, Lambert RM (1985) J Catal 93:92
18. Grant RB, Lambert RM (1985) Langmuir 1:29
19. Tan SA, Grant RB, Lambert RM (1986) J Catal 100:383
20. Tan SA, Grant RB, Lambert RM (1987) J Catal 106:54
22. Linic S (2003) PhD Dissertation, University of Delaware
23. Jones GS, Mavrikakis M, Barteau MA, Vohs JM (1998) J Am Chem Soc 120:3196

24. Wu G, Stacchiola D, Kaltchev M, Tysoe WT (2000) Surf Sci 463:81
25. Lukaski AC, Enever MCN, Barteau MA (2007) Surf Sci 601:3372
26. Force EL, Bell AT (1975) J Catal 38:440
27. Bare SR (1992) J Vac Sci Technol A 10:2336
28. Liu XY, Klust A, Madix RJ, Friend CM (2007) J Phys Chem C 111:3675
29. Kokalj A, Gava P, De Gironcoli S, Baroni S (2008) J Phys Chem C 112:1019
30. Bocquet ML, Loffreda D (2005) J Am Chem Soc 127:17207
31. Ko EI, Benziger JB, Madix RJ (1980) J Catal 62:264
32. Baerends EJ (1999) ADF Version 1999.02
33. Baerends EJ, Ellis DE, Ros P (1973) Chem Phys 2:41
34. Baerends EJ, Ros P (1978) Int J Quantum Chem Symp 12:169
35. Wu K, Wang DZ, Wei XM, Cao YM, Guo XX (1994) Sci China Ser B Chem 37:1045
36. Guo XC, Madix RJ (2001) J Phys Chem B 105:3878
37. Barteau MA, Bowker M, Madix RJ (1981) J Catal 67:118
38. Sault AG, Madix RJ (1986) Surf Sci 172:598
39. Stacchiola D, Wu G, Kaltchev M, Tysoe WT (2001) Surf Sci 486:9
40. Backx C, De Groot CPM, Biloen P (1980) Appl Surf Sci 6:256
41. Bocquet ML, Michaelides A, Loffreda D, Sautet P, Alavi A, King DA (2003) J Am Chem Soc 125:5620
42. Backx C, De Groot CPM, Biloen P, Sachtler WHM (1983) Surf Sci 128:81